COBEM 99
XV Congresso Brasileiro de Engenharia Mecânica
15th Brazilian Congress of Mechanical Engineering
22 - 26 de Novembro de 1999 / November 22 - 26, 1999 Águas de Lindóia, São Paulo,

TWO-DIMENSIONAL CONJUGATE HEAT TRANSFER IN A FLAT PLATE SOLAR COLLECTOR

Juliano Duarte
Edson Luiz Zaparoli
CTA – ITA – Departamento de Energia
Pça. Mal. Eduardo Gomes, 50 – Vila das Acácias
CEP: 12228-900 – São José dos Campos – SP – Brasil

Summary. *In this work, the effects of a two-dimensional convection and conduction conjugate heat transfer on a cross section of a flat plate solar collector are investigated. Through the finite element method, a simultaneous solution of momentum and energy equations for analysis of the heat exchange in the fluid (water) and in the solid (absorber plate, back insulation and ducts) is obtained. The results are compared to the one-dimensional uncoupled formulation used in the design of solar collectors, for different values of the tube thermal conductivity and the distance between the tubes. This analysis allows the evaluation of the error due to the assumption made in the one-dimensional uncoupled formulation for the determination of useful energy gain per unit of collector length and for the collector efficiency.*

Keywords: *Conjugate Heat Transfer, Finite Element Method, Solar Collectors.*

1. INTRODUCTION

In general, a solar collector is a heat exchanger that transforms solar radiant energy into useful heat. The incident solar heat absorbed above the absorber plate is transferred by conduction to the tube and by convection to the fluid. As pointed out by Duffie and Beckman (1980), flat plate collectors can be designed for applications requiring energy delivery at moderate temperatures, up to about 100^{o}C above ambient temperature, and they are used efficiently in the solar water heating, whereas potential uses include building air conditioning and industrial process heating.

In many practical design situations, the formulations of collector performance are reduced to relatively simple forms. In this case, a one-dimensional analytical model is used to deal with the problem of heat conduction in the absorber plate, insulation and ducts. The tube wall resistance may be neglected, and the interactions of the convection heat transfer between the tube and the fluid are represented taking into account a uniform convection coefficient for the entire interface solid-fluid. This one-dimensional uncoupled model still considers constant temperature in the tube internal surface.

Concerning this aspect, the two-dimensional heat transfer analysis with a conjugate approach, Patankar (1980), in which the conduction in the solid and the convection in the fluid are considered in a single calculation domain, becomes necessary to evaluate when the assumption made in the one-dimensional analysis is valid and then predict the performance of the collector more accurately.

In recent years, with the availability of high-speed and large-capacity digital computers, numerical methods and the Computational Fluid Dynamics (CFD) codes have been brought out to solve heat transfer and fluid mechanic problems in engineering application, Freitas (1995).

In this context, this work uses a computational program based on the finite element method for the study of conduction and convection effects in the two-dimensional conjugate heat transfer in a cross-section of a flat plate solar collector. This solar collector is composed by an absorber plate, back insulation and tubes. The results are compared to the one-dimensional uncoupled model found in literature.

2. TWO-DIMENSIONAL CONJUGATE HEAT TRANSFER FORMULATION

In the two-dimensional conjugate heat transfer approach, the conduction in the solid and the convection in the fluid must both be considered, with a proper matching at the fluid-solid interface, and achieving a simultaneous solution of the momentum and energy equations. The adherence conditions of the fluid lying in the solid region and the equality of temperature and heat flux in the interface are intrinsic to the model. A scheme of the collector is shown in Fig. 1, where W is the distance between the tubes; e_p is the plate thickness, e_i is the insulation thickness; D and d are the external and internal diameters of the tube, respectively.

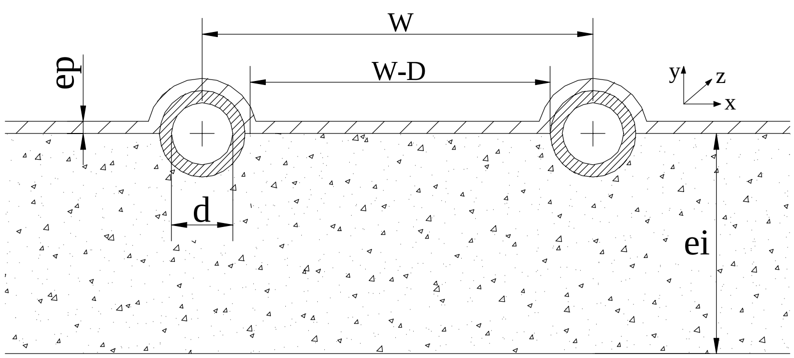

Figure 1: Cross-section of a basic flat plate solar collector.

The momentum and energy equations are presented in the following section in the Cartesian coordinate system, for steady state and constant properties, as well as the boundary conditions associated with the problem.

2.1 Velocity Field

The momentum equation in the flow direction for laminar forced convection inside a circular tube, in which it is considered that the flow is hydrodynamically developed, can be written in the form:

$$\mu\left(\frac{\partial^2 u}{\partial x^2}+\frac{\partial^2 u}{\partial y^2}\right)=\frac{dP}{dz} \tag{1}$$

where μ is the dynamic viscosity of the fluid, u is the velocity and dP/dz is the constant axial pressure gradient.

Equation (1) will be solved in a domain shown in Fig. 2. In the solid region, *dP/dz=0* and a very high value of viscosity with respect to the fluid viscosity are adopted, Patankar (1980).

After the solution of Eq. (1), the following flow parameters can be obtained:

- Mean velocity:

$$U_b = \frac{1}{A} \iint u \, dxdy \tag{2}$$

where A is the tube cross-section area.

- Reynolds number:

$$\mathrm{Re} = \frac{\rho \, U_b \, d}{\mu} \tag{3}$$

where ρ is the density of the fluid.

- Friction factor:

$$f = - {dP}/{dz} \left(\frac{2\,d}{\rho \, U_b^{\;2}} \right) \tag{4}$$

2.2 Temperature Field

The energy equation in the thermally fully developed region, assuming a very small axial diffusive transport compared to the radial diffusive transport, and considering that the tube wall mean temperature is uniform in the axial direction, Kays and Crawford (1993), is given by:

$$k \left(\frac{\partial^2 T}{\partial x^2} + \frac{\partial^2 T}{\partial y^2} \right) = \rho \, cp \, u \left(\frac{T_{wm} - T}{T_{wm} - T_b} \right) \frac{dT_b}{dz} \tag{5}$$

where k is the thermal conductivity and c_p is the specific heat.

Equation (5) also will be solved in the domain shown in Fig. 2. In the solid region (u=0), the right side of Eq. (5) becomes equal to zero and the energy equation is simplified to the two-dimensional, steady state heat conduction equation with no heat generation.

With the results of Eqs. (1) and (5), the following parameters concerning to the heat transfer in the fluid can be calculated:

- Bulk temperature:

$$T_b = \frac{1}{A \, U_b} \iint u \, T \, dxdy \tag{6}$$

- Tube wall mean temperature:

$$T_{wm} = \frac{1}{Per} \oint_s T_w \, ds \tag{7}$$

where Per is the perimeter, T_w is the wall temperature and s is the arc length on the tube internal surface.

- Heat flux from the tube to the fluid:

$$qu'' = -k_t \vec{\nabla} T . \overrightarrow{n_1} \Big|_{wall} \tag{8}$$

where k_t is the thermal conductivity of the tube and $\vec{n}_1$ represents the normal unit vector at the internal surface and outward to the fluid region.

- Useful energy gain per unit of collector length:

$$qu' = \oint_s - k_t \vec{\nabla} T . \overrightarrow{n_1} \, ds \tag{9}$$

- Axial mean temperature gradient:

$$\frac{dT_b}{dz} = \frac{\oint_s - k_t \vec{\nabla} T . \vec{n}_1 \, ds}{\rho \, c_p U_b \, A} \tag{10}$$

- Local convection coefficient:

$$h = \frac{- k_t \vec{\nabla} T . \overrightarrow{n_1} \Big|_{wall}}{T_w - T_b} \tag{11}$$

- Mean convection coefficient:

$$\bar{h} = \frac{\oint_s - k_t \vec{\nabla} T . \overrightarrow{n_1} \, ds}{Per \left(T_{wm} - T_b \right)} \tag{12}$$

- Mean Nusselt number:

$$\overline{Nu} = \frac{\bar{h} \, d}{k_f} \tag{13}$$

where k_f is the thermal conductivity of the fluid.

2.3 Boundary Conditions

The boundary conditions associated to the momentum and the energy equations are applied on the domain represented in Fig. 2 and given by:

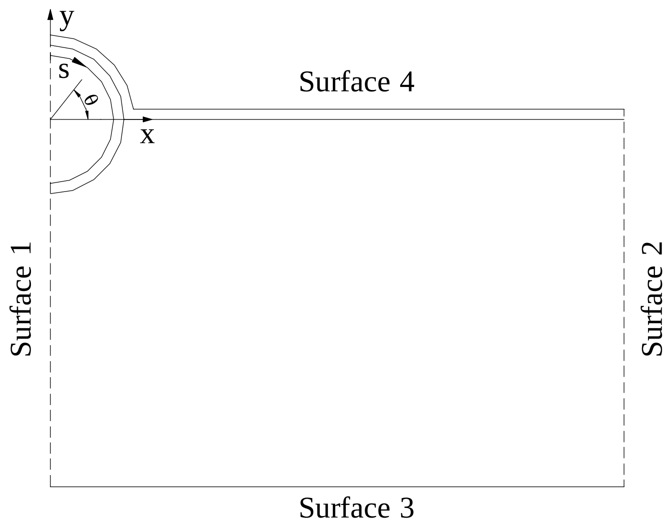

Figure 2: Symmetrical cross-section of the studied collector.

Surface 1: Symmetry.

$$\begin{aligned} &u = 0, \text{ zero velocity on the solid} \\ &\partial u / \partial n_2 = 0, \text{ simmetry line on the fluid} \\ &\partial T / \partial n_2 = 0, \text{ simmetry line on the solid and fluid} \end{aligned} \qquad (14)$$

Surface 2: Symmetry.

$$\begin{aligned} &u = 0, \text{ zero velocity on the solid} \\ &\partial T / \partial n_2 = 0, \text{ Simmetry line on the solid} \end{aligned} \qquad (15)$$

Surface 3: Bottom of the collector.

$$\begin{aligned} &\mathrm{u} = 0, \text{ zero velocity on the solid} \\ &k_i \, \partial T / \partial n_2 = -h_a \left(T - T_a\right), \text{ bottom convective heat loss} \end{aligned} \qquad (16)$$

Surface 4: Top of the collector.

$$\begin{aligned} &u = 0, \text{ zero velocity on the solid} \\ &k_p \, \partial T / \partial n_2 = S - U_c \left(T - T_a\right), \text{ top heat gain} \\ &k_p \, \partial T / \partial n_2 = S \cos\left(90 - \theta\right) - U_c \left(T - T_a\right), \text{ top heat gain} \end{aligned} \qquad (17)$$

where n_2 represents the normal unit vector outward to the domain surface, k_i is the thermal conductivity of the insulator, k_p is the thermal conductivity of the flat plate, T_a is the ambient temperature, h_a is the free convection coefficient to the atmosphere, S is the absorbed solar energy incident on the flat plate and U_c is the overall thermal loss coefficient of the collector.

3. NUMERICAL SOLUTION

The numerical solution of the momentum and the energy equations was obtained by using a program based upon the Galerkin finite element method. This program uses a quadratic interpolation polynomial to convert continuous partial differential equations into discrete nodal equations. The program also uses an unstructured automated adaptive grid refinement, fine gridding only in areas involving sharp curvatures, tight geometries and large gradient of dependent temperature as needed until error criteria are met, providing near optimum speed and memory utilization. The algebraic equations system has been solved through the iterative conjugate-gradient method, using the incomplete Cholesky decomposition as a preconditioner, Macsyma Inc. (1996).

4. ONE-DIMENSIONAL UNCOUPLED FORMULATION

In accordance with Bliss (1959), the efficiency of a collector is directly proportional to a "collector efficiency factor" F'. For the collector shown in Fig. 1, this collector efficiency factor is given by:

$$F' = \frac{1}{\dfrac{W}{D + (W - D)F} + \dfrac{W\,U_c}{\pi\, d\, h}} \tag{18}$$

The two terms in the denominator of Eq. (18) relate to the heat conduction from the absorber plate to the tubes and the heat transfer from the internal tube surface to the fluid, respectively.

The fin (flat plate) efficiency F is:

$$F = \frac{\tanh\left[\sqrt{\dfrac{U_c}{k_p\, e_p}}\left(\dfrac{W - D}{2}\right)\right]}{\sqrt{\dfrac{U_c}{k_p\, e_p}}\left(\dfrac{W - D}{2}\right)} \tag{19}$$

The useful energy gain per unit of collector length is given by:

$$qu' = W\,F'\left[S - U_c\,(T_b - T_a)\right] \tag{20}$$

The collector efficiency is given by:

$$\eta = \frac{qu'}{S\,W} \tag{21}$$

In this one-dimensional approach, the tube wall resistance is neglected and the analysis of convection inside the tube is depicted by a uniform coefficient at the tube internal surface.

5. RESULTS AND DISCUSSION

In this work, the following numerical values for the water physical properties are used: ρ = 985 kg/m^3, k_f = 0,651 W/(m·K), c_p = 4184 kJ/(kg·K), μ = 7,71 $\times 10^{-4}$ kg/(m·s). The values for the other parameters are: U_c = 7 W/(m^2·K), S = 1100 W/m^2, h_a = 10 W/(m^2·K), T_b = 333 K, T_a = 293 K, dp/dz = 10 kg/(m^2·s^2), k_p = 211 W/(m·K), k_t = 211 W/(m·K), k_i = 0,024 W/(m·K), e_p = 0,001 m, e_i = 0,050 m, d = 0,010 m, D = 0,013 m, W = 0,120 m.

The value of the axial mean temperature gradient was estimated initially and improved after each iteration until the convergence criteria is obtained.

The numerical results obtained for the product of the friction factor and the Reynolds number ($f \cdot Re$) and for the mean Nusselt number ($\overline{Nu}$) are in very good agreement with the ones presented by Kays and Crawford (1993) for constant wall temperature boundary condition, despite the fact of variable temperature in the tube internal wall surface, as shown in Fig. 3.

We can observe in Fig. 3 higher values of temperature in the region in contact with the flat plate, due to solar energy absorption, and lower values of temperature in the region in contact with the back insulator, due to losses by conduction.

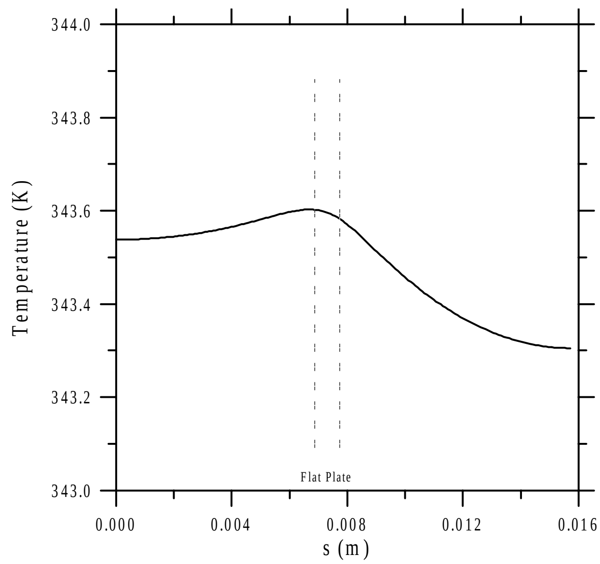

Figure 3: Temperature distribution in the tube internal wall surface.

Figure 4 shows that the temperature in the collector cross-section (along the *x* axis in Fig. 2) decreases from the flat plate symmetry line to the region near the tube, remaining practicality constant in the tube wall and decaying in the fluid region.

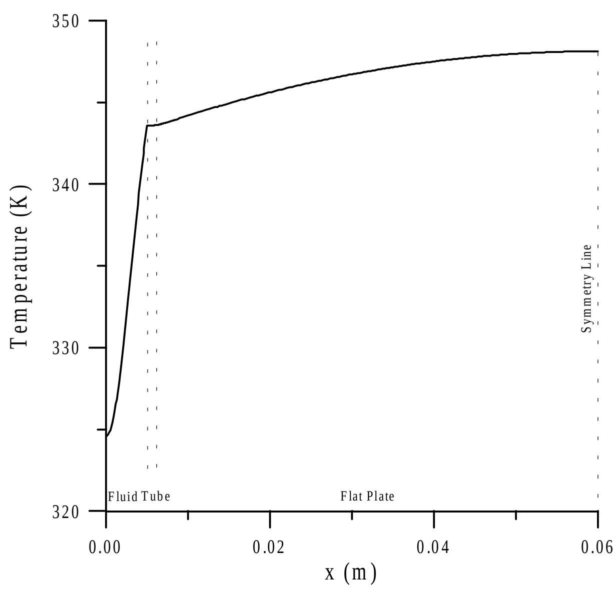

Figure 4: Temperature distribution in the cross-section of the collector.

The isothermal lines and the temperature gradient vectors in Fig. 5 show that the heat conduction has more intense two-dimensional features in the region next to the tube (Fig. 5b) and in the region near the flat plate symmetry line (Fig. 5c). These evidences of two-dimensional conduction are fundamental for the more realistic analysis of the thermal behavior of the collector.

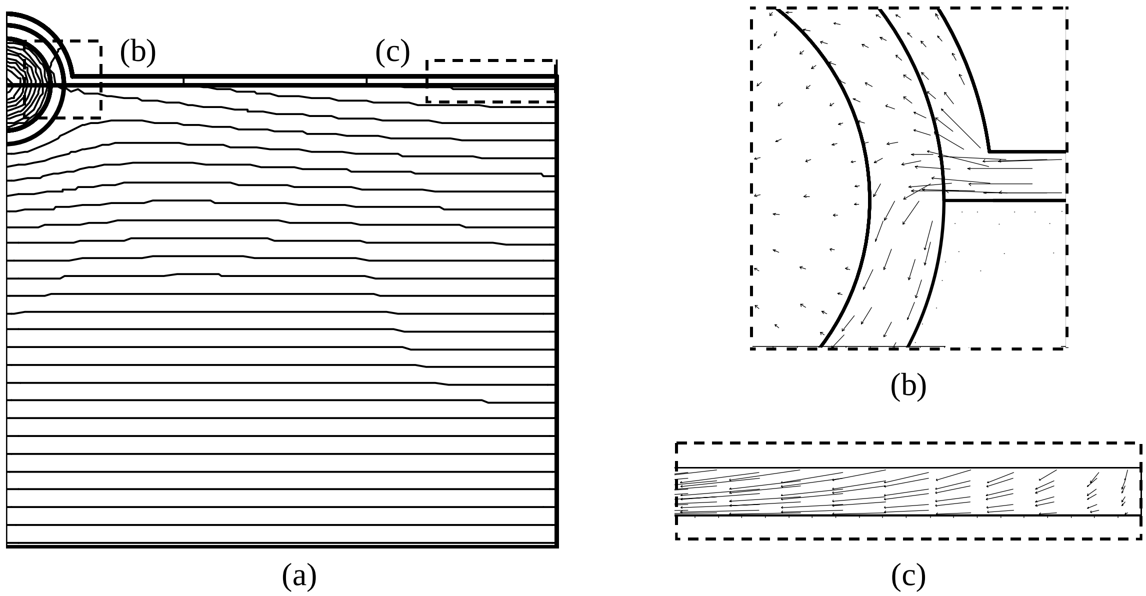

Figure 5: (a) Isothermal lines in the cross-section of the collector, (b) Two-dimensional heat flux in the tube, (c) Two-dimensional heat flux in the flat plate.

Results for the useful energy gain and for the collector efficiency. The results obtained from Eq. (9) have been compared to the results of Eq. (20) for different values of tube thermal conductivity and tube spacing. Through the data obtained for the useful energy gain, we can also compare the results for the collector efficiency defined in Eq. (27).

Figure 6 shows that the error between one-dimensional and two-dimensional formulations decreases with the increase of the tube thermal conductivity, being around 6% for values above the 150 W/(m·K). For values of thermal conductivity below that, the tube wall resistance starts to be an important factor in the formulation. Thus, the two-dimensional approach becomes essential for a more accurate analysis of the collector performance.

Figure 7 shows that the error between the one-dimensional and two-dimensional formulations also diminishes with the increase of tube spacing, practically being constant for values above W=0,120 m, due to the predominance of the one-dimensional conduction in the flat plate.

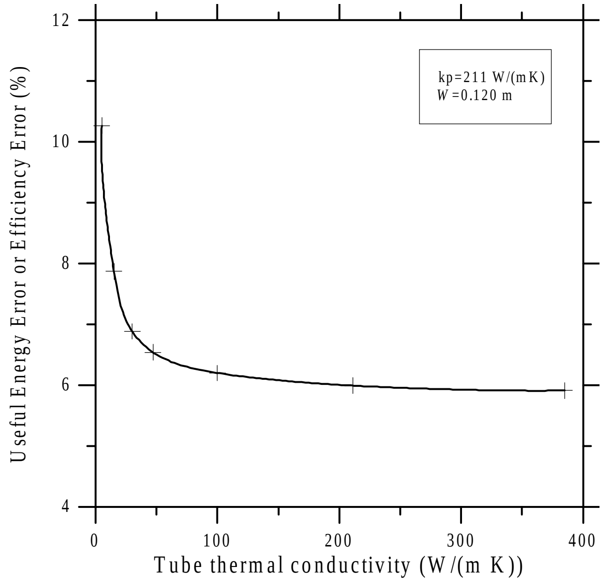

Figure 6: Useful energy gain and collector efficiency error variation with tube wall thermal conductivity.

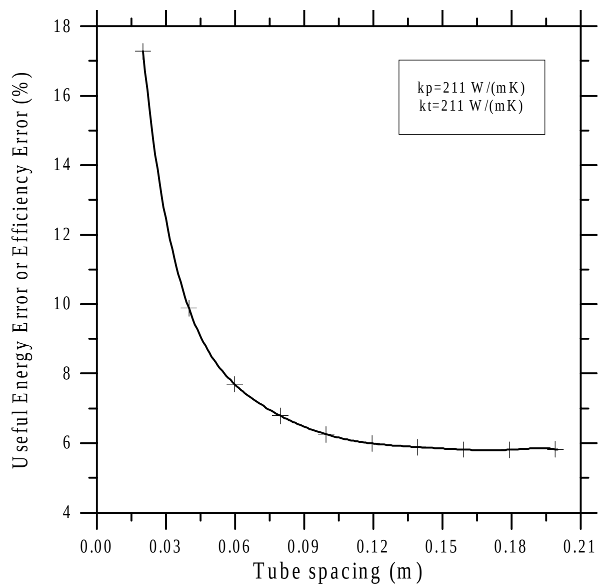

Figure 7: Useful energy gain and collector efficiency error variation with tube spacing.

6. CONCLUDING REMARKS

The thermal and hydrodynamic behavior of a flat plate solar collector was studied using a finite element method with a conjugate heat transfer approach, where the conduction in the solid and the convection in the fluid were analyzed in a coupled form. The numerical solution has presented no convergence or stability problems, and the mesh used was refined in the regions where the variable presented greater gradients, *i.e.*, near the absorber flat plate region and near the tube-water interface. The numerical results obtained were compared with the results of the classic formulation, which assumes one-dimensional heat conduction and tube wall resistance negligible. With the two-dimensional conjugate heat transfer, it was verified that the heat conduction presents more intense two-dimensional features near the tube region and near the symmetry line of the absorber plate. Thus, the main sources of error were found for short flat plate and for lower values of tube thermal conductivity.

7. ACKNOWLEDGEMENTS

The first author is grateful for the grant and all the support provided by CAPES.

8. REFERENCES

Bliss, R. W. Jr., 1959, The Derivations of Several Plate-Efficiency Factors Useful in the Design of Flat-Plate Solar Heat Collectors, Solar Energy, vol. 3, pp. 55-64.

Duffie, J. A. and Beckman, W. A., 1980, Solar Engineering of Thermal Processes, J. Wiley, New York.

Freitas C. J., 1995, Perspective: Selected Benchmarks from Commercial CFD Codes, Trans. ASME Journal of Fluids Engineering, vol. 117, pp. 206-218.

Kays, W. M. and Crawford, M. E., 1993, Convective Heat and Mass Transfer, McGraw-Hill, 3rd. ed., New York.

Macsyma Inc., 1996, PDEase2D™ 3.0 Reference Manual, 3rd. Ed.

Patankar, S. V., 1980, Numerical Heat Transfer and Fluid Flow, Hemisphere Publishing Corporation, Washington.